An Internal Model Control Strategy for Nonlinear Systems

Michael A. Henson and Dale E. Seborg

Dept. of Chemical and Nuclear Engineering, University of California, Santa Barbara, CA 93106

An internal model control (IMC) strategy for nonlinear single-input single-output systems is proposed. The controller is designed to provide nominal performance, and a nonlinear filter is added to make the controller implementable and to account for plant/model mismatch. An important advantage of the new approach is that the assumption of full-state feedback inherent in most input-output linearization schemes is eliminated. However, the proposed IMC strategy is restricted to open-loop stable systems with stable inverses. Under mild assumptions, the closed-loop system possesses the same stability, perfect control, and zero offset properties as linear IMC. Simulation results for a continuous fermentor illustrate the advantages of the nonlinear IMC strategy.

Introduction

Internal model control (IMC) is a powerful controller design strategy for linear systems described by transfer function models (Morari and Zafiriou, 1989). For open-loop, stable systems, the IMC approach provides a very simple parameterization of all stabilizing controllers. The IMC factorization procedure provides valuable insights into the inherent control limitations presented by particular models. Due to the IMC structure, integral action is included implicitly in the controller. Moreover, plant/model mismatch can be addressed via the design of a robustness filter.

Unfortunately, virtually all real processes are nonlinear. Some are sufficiently linear in the region of operation so that conventional PID controllers provide adequate performance. But, for highly nonlinear processes, conventional feedback controllers must be detuned significantly to ensure stability.

Therefore, performance is often severely degraded. Model-based control strategies for nonlinear processes usually require local linearization and linear controller design based on the linearized model. This approach, however, may not be successful when the process is highly nonlinear or deviates significantly from the operating point where the model was linearized. For batch and semibatch processes, it is difficult to define an operating point for linearization. Since reasonably accurate nonlinear models are available for a variety of processes, control strategies in which the nonlinear process model serves as the basis for controller design can be expected to yield significantly improved performance.

In this article, an IMC strategy for nonlinear single-input single-output (SISO) systems is proposed. Unlike existing nonlinear controller design techniques that incorporate IMC con-

cepts, the new approach is a general extension of linear IMC to open-loop, stable, nonlinear systems with stable inverse. The nonlinear process model is used directly in the design of the controller, and a nonlinear filter is added to make the controller implementable and improve robustness. Unlike most input-output linearization techniques, full-state feedback is not required since the process model functions as an open-loop observer. If the model satisfies mild assumptions, the closed-loop system possesses the same stability, perfect control, and zero offset properties as linear IMC. A linear process model is used to compare the new approach to linear IMC, and extensions for nonlinear systems with disturbances are proposed. Simulation results for a continuous fermentor demonstrate that the nonlinear IMC strategy is superior to PI control and compares favorably to exact linearization based on full-state feedback even if significant modeling errors are present.

Existing Approaches to Nonlinear Internal Model Control

The development of a general nonlinear extension of IMC poses serious difficulties due to the inherent complexity of nonlinear systems. For instance, except for very simple SISO systems (Kravaris and Daoutidis, 1990), the IMC factorization procedure has no well-defined nonlinear analog. Also, very few tools exist for the design and analysis of robust nonlinear controllers. Furthermore, linear IMC is based on transfer functions models, while nonlinear systems are usually described by nonlinear state-space models. Despite these difficulties, several nonlinear controller design techniques that incorporate concepts from linear IMC have been developed recently. In this section, these design methods are reviewed, and it is shown that a general IMC design strategy for nonlinear systems has not yet been developed. Other types of nonlinear controller design strategies for process control have been reviewed by Kravaris and Kantor (1990a,b) and Henson and Seborg (1991).

Economou et al. (1986) proposed an IMC strategy for open-loop, stable, nonlinear systems with stable inverses. Input-output operators were used to show that their nonlinear IMC technique satisfies the same stability, perfect control, and zero offset properties as linear IMC. The controller was based on the inverse of the nonlinear model, and a filter was added to account for input constraints and modeling errors. The stability of the model inverse was analyzed using the small gain theorem. Because the calculation of the required nonlinear gains is nontrivial (Nikolaou and Manousiouthakis, 1989), the stability theorems are difficult to use in practice. Although an input-output approach was used for analysis, the only analytical technique investigated for construction of the model inverse was the state-space approach of Hirschorn (1979). However, the Hirschorn inverse is internally unstable due to pole-zero cancellations at the origin (Kravaris and Kantor, 1990a,b).

Economou et al. (1986) augmented the nonlinear controller with a linear filter because design techniques for nonlinear filters that preserve the nominal stability and no offset properties were not available. Because linear filters do not affect the stability of the controller, the resulting closed-loop performance was unacceptable. Hence, the model inverse was constructed using numerical procedures based on the contraction mapping principle and Newton's method. The Newton

procedure was reliable and efficient, but requires the solution of a linear variational problem. This numerical approach to nonlinear IMC is, therefore, computationally-intensive. Moreover, analysis of the resulting iterative procedure is difficult (Economou and Morari, 1985; Li et al., 1990). Since disturbances were treated as modeling errors, no explicit techniques were proposed to incorporate measured disturbances in a feedforward/feedback control scheme.

The nonlinear inferential control (NIC) strategy proposed by Parrish and Brosilow (1986, 1988) is an extension of linear inferential control (Joseph and Brosilow, 1978). As in other IMC approaches, the difference between the plant and model outputs is used as a feedback signal. An estimator provides the nonlinear controller with state and parameter estimates, and a linear filter is used to define a reference trajectory for the closed-loop system. The most significant limitation of the NIC strategy is that very few quantitative design guidelines are provided for the controller and estimator. Additionally, discretization is often required since a discrete-time approach is employed. The effects of model discretization on stability and performance were not reported. Despite these limitations, the NIC approach has been successfully applied to several nonlinear process models, including an open-loop, unstable, styrene polymerization reactor (Hidalgo and Brosilow, 1990).

Calvet and Arkun (1988) used an IMC scheme to implement their state-space linearization approach for nonlinear systems with disturbances. A disadvantage of the state-space linearization approach is that an artificial controlled output is introduced in the controller design procedure and cannot be specified *a priori* (Kantor and Kravaris, 1990a,b; Henson and Seborg, 1991). Another disadvantage of this method is that the nonlinear controller requires state feedback. An alternative IMC strategy for nonlinear systems has been proposed by Alvarez and Alvarez (1989). The tracking and regulation behavior of the closed-loop system can be specified independently via two reference models. Hence, the approach is similar to the two-degree-of-freedom controller developed for linear IMC (Morari and Zafiriou, 1989). Additionally, state feedback is not required because the process model acts as an open-loop observer. However, a linear map between the setpoint and output is not usually obtained since an artificial output is controlled. Thus, it is difficult to design reference models to satisfy specific performance criteria. Bartusiak et al. (1989) and Bartee et al. (1989) have used the reference system synthesis technique to design IMC-equivalent controllers for first- and second-order linear systems. However, no extensions for nonlinear systems are presented.

All the nonlinear controller design techniques discussed above incorporate some aspects of linear IMC. These methods, however, do not represent a satisfactory extension of IMC to nonlinear systems. In this article, a general extension of linear IMC to single-input, single-output nonlinear systems is presented. Like the nonlinear IMC approach of Economou et al. (1986), the proposed strategy is restricted to open-loop, stable systems with stable inverses. The new IMC approach, however, is much easier to implement than the method of Economou et al. (1986). To take advantage of recent results in nonlinear control theory (Isidori, 1989), a state-space approach is employed. A stable and implementable IMC controller is obtained by augmenting a model inverse controller with a nonlinear filter. Hence, the IMC controller can be represented analytically, and compu-
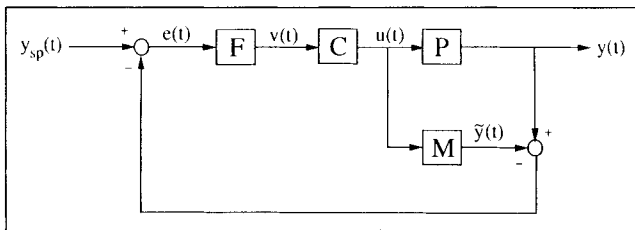
Figure 1. General structure of nonlinear internal model control.

tationally-intensive numerical procedures are not required. A simple and useful characterization of model inverse stability is developed. Finally, the effects of disturbances are considered explicitly. For measured disturbances that satisfy a matching condition, feedforward/feedback controllers are constructed.

An Internal Model Control Strategy for Nonlinear Systems

We first consider the control of nonlinear single-input single-output systems without disturbances. Extensions for systems with disturbances are discussed later. Assume that the model M available for controller design has the form

$$\dot{\tilde{x}} = \tilde{f}(\tilde{x}) + \tilde{g}(\tilde{x})u \qquad (1)$$
$$\tilde{y} = \tilde{h}(\tilde{x})$$

where $\tilde{x}$ is an $\tilde{n}$-dimensional state vector, u is a scalar manipulated input, $\tilde{y}$ is a scalar controlled output, $\tilde{f}(\tilde{x})$ and $\tilde{g}(\tilde{x})$ are $\tilde{n}$-dimensional vector functions, and $\tilde{h}(\tilde{x})$ is a scalar output function.

The plant P is assumed to have the form,

$$\dot{x} = f(x) + g(x)u \qquad (2)$$
$$y = h(x)$$

where x is an n-dimensional state vector, y is a scalar controlled output, and the nonlinear functions $f(x)$, $g(x)$, and $h(x)$ are defined similarly to the functions in M. Although M and P are affine (linear) in the manipulated input u, the proposed IMC strategy can be extended to nonaffine models using the implicit function theorem (Henson and Seborg, 1990b). The functions, $f(x)$, $g(x)$, and $h(x)$, may differ from the corresponding functions in the model. Hence, the plant/model description can include structural uncertainties and/or unmodeled dynamics. Even if the nonlinear functions are identical, the model state $\tilde{x}$ may be different from the plant state x if the model is not properly initialized.

As suggested by Economou et al. (1986), the nonlinear IMC structure can be represented as in Figure 1 where C is a nonlinear controller and F is a robustness filter. The nonlinear IMC controller Q is defined as the composition of C and F:

$$Q \triangleq CF \qquad (3)$$

The design of the nonlinear controller C and filter F is discussed in the following sections.

Controller design

As in linear IMC (Morari and Zafiriou, 1989), the first objective is to design the controller C such that the closed-loop system is stable if a perfect model is available (nominal stability). The nominal stability problem is considered in the section on the Properties of the Closed-Loop System. The next objective is to design C such that a performance criterion is satisfied if the model is perfect (nominal performance). Thus, the following assumption is invoked temporarily.

Assumption 1: The model is perfect $(M \equiv P)$. Note that assumption 1 implies that $\tilde{f} = f$, $\tilde{g} = g$, $\tilde{h} = h$, and $\tilde{x}(0) = x(0)$. At this point, we assume that the filter is the identity operator: $F = 1$. In the following section, assumption 1 will be relaxed by augmenting C with the filter F. The controller C is chosen to minimize the tracking error,

$$\min_C \| y_{sp}(t) - y(t) \| \qquad (4)$$

where $\| \ \|$ represents a suitable norm and $y_{sp}(t)$ is the setpoint. The feedback signal to C,

$$e \triangleq y_{sp} - y + \tilde{y} \qquad (5)$$

simplifies to $e = y_{sp}$ by assumption 1. Hence, the plant output can be expressed as:

$$y = PCFe = MCy_{sp} \qquad (6)$$

Using Eq. 6, the tracking error can be written as,

$$y_{sp} - y = y_{sp} - MCy_{sp} = (1 - MC)y_{sp} \qquad (7)$$

and the optimization problem in Eq. 4 becomes:

$$\min_C \| (1 - MC)y_{sp} \| \qquad (8)$$

The performance criterion in Eq. 8 is zero for any norm and any setpoint if the controller C is chosen to be the right inverse of the model:

$$C = M_r^{-1} \qquad (9)$$

From Eq. 6 it is clear that this choice of C provides "perfect" control: $y(t) = y_{sp}(t)$ for all $t > 0$.

As in the nonlinear IMC approach of Economou et al. (1986), the model inverse is constructed using the method of Hirschorn (Hirschorn, 1979; Kravaris and Kantor, 1991a,b). To ensure that the model inverse is a well-defined dynamical system, a standard smoothness assumption is required (Boothby, 1986; Isidori, 1989).

Assumption 2: The vector fields $\tilde{f}(\tilde{x})$ *and* $\tilde{g}(\tilde{x})$ *and scalar field* $\tilde{h}(\tilde{x})$ *are of class* C^∞ (*i.e., they have continuous derivatives of all order*). Note that assumption 2 implies that all derivatives of $\tilde{f}(\tilde{x})$, $\tilde{g}(\tilde{x})$, and $\tilde{h}(\tilde{x})$ are bounded. Fortunately, most systems of interest in process control satisfy assumption 2.

At this point, it is useful to introduce some notation from differential geometry (Boothby, 1986; Kravaris and Kantor, 1990a,b). The *Lie derivative* of a scalar function $\bar{h}(\tilde{x})$ with respect to a vector function $\tilde{f}(\tilde{x})$ is defined as:

$$L_{\tilde{f}}\bar{h}(\tilde{x}) \triangleq \frac{\partial \bar{h}}{\partial \tilde{x}}\tilde{f}(\tilde{x}) \qquad (10)$$

Higher-order Lie derivatives can be defined recursively as,

$$L_{\tilde{f}}^k\bar{h}(\tilde{x}) \triangleq \sum_{j=1}^n \frac{\partial}{\partial \tilde{x}_j}\{L_{\tilde{f}}^{k-1}\bar{h}(\tilde{x})\}\tilde{f}_j(\tilde{x}) \qquad (11)$$

where

$$L_{\tilde{f}}^0\bar{h}(\tilde{x}) \triangleq \bar{h}(\tilde{x}) \qquad (12)$$

The input in Eq. 1 is said to have *relative degree r* at a point $\tilde{x}_o$ if

(i) $L_{\tilde{g}}L_{\tilde{f}}^k\bar{h}(\tilde{x}) = 0$

$\forall$ x in a neighborhood of $\tilde{x}_o$ and $\forall$ $k < r-1$ (13)

(ii) $L_{\tilde{g}}L_{\tilde{f}}^{r-1}\bar{h}(\tilde{x}_o) \neq 0$ (14)

The relative degree represents the number of times the model output $\tilde{y}$ must be differentiated with respect to time so that the input u appears explicitly. The relative degree of a linear system is the difference between the orders of the denominator and numerator polynomials. Hence, the relative degree provides a measure of "properness." This property is exploited in the filter design discussed later.

Unfortunately, some systems have *singular points* where the relative degree is not well defined (Isidori, 1989; Henson and Seborg, 1990a). To avoid singularities in the control law, the relative degree is assumed to be constant throughout the entire state space.

Assumption 3: $L_{\tilde{g}}L_{\tilde{f}}^{r-1}\bar{h}(\tilde{x}) \neq 0$ $\forall$ $\tilde{x} \in R^{\tilde{n}}$. Note that assumption 3 implies that the steady-state gain of the model cannot change sign. Although this assumption is not often stated explicitly, it is required in almost all nonlinear control strategies based on exact linearization (Kravaris and Chung, 1987; Lee and Sullivan, 1988; Bartusiak et al., 1989). Recent results indicate that this assumption can be relaxed if the model is "approximately" inverted (Kappos, 1989; Lien and Wang, 1990).

By assumption 3, the first r time derivatives of the model output can be represented as:

$$\tilde{y}^{(k)} = L_{\tilde{f}}^k\bar{h}(\tilde{x}) \quad 1 \leq k \leq r-1 \qquad (15)$$

$$\tilde{y}^{(r)} = L_{\tilde{f}}^r\bar{h}(\tilde{x}) + L_{\tilde{g}}L_{\tilde{f}}^{r-1}\bar{h}(\tilde{x})u \qquad (16)$$

where

$$\tilde{y}^{(k)} \triangleq \frac{d^k}{dt^k}\tilde{y}(t) \qquad (17)$$

The Hirschorn inverse (1979) is obtained by solving Eq. 16 for the input u and substituting the result in Eq. 1:

$$\dot{\tilde{x}} = \tilde{f}(\tilde{x}) - \frac{L_{\tilde{f}}^r\bar{h}(\tilde{x})}{L_{\tilde{g}}L_{\tilde{f}}^{r-1}\bar{h}(\tilde{x})}\tilde{g}(\tilde{x}) + \frac{\tilde{g}(\tilde{x})}{L_{\tilde{g}}L_{\tilde{f}}^{r-1}\bar{h}(\tilde{x})}\tilde{y}^{(r)} \qquad (18)$$

$$u = -\frac{L_{\tilde{f}}^r\bar{h}(\tilde{x})}{L_{\tilde{g}}L_{\tilde{f}}^{r-1}\bar{h}(\tilde{x})} + \frac{1}{L_{\tilde{g}}L_{\tilde{f}}^{r-1}\bar{h}(\tilde{x})}\tilde{y}^{(r)} \qquad (19)$$

Thus, the model inverse reconstructs the input $u(t)$ from the rth derivative of the output $\tilde{y}^{(r)}(t)$. Note that the Hirschorn inverse is a nonminimal realization of the model inverse since it is an n-dimensional system. Minimal realizations can be also derived (Kravaris and Kantor, 1990a). To track the setpoint, the model inverse controller C can be chosen as in Eq. 19 with $y_{sp}^{(r)}$ as the input:

$$u = -\frac{L_{\tilde{f}}^r\bar{h}(\tilde{x})}{L_{\tilde{g}}L_{\tilde{f}}^{r-1}\bar{h}(\tilde{x})} + \frac{1}{L_{\tilde{g}}L_{\tilde{f}}^{r-1}\bar{h}(\tilde{x})}\tilde{y}_{sp}^{(r)} \qquad (20)$$

The model inverse controller in Eq. 20 does not require state feedback from the plant since the model acts as an open-loop observer. The following assumption is required to ensure that the state estimates of the open-loop observer converge to the plant state if the observer is improperly initialized.

Assumption 4: For every constant input u_o, the model in Eq. 1 has a globally asymptotically stable equilibrium point $\tilde{x}_o$. Assumption 4 implies that each equilibrium point is stable and there is a single equilibrium point for each constant input. Hence, the proposed IMC strategy is restricted to open-loop, stable systems with a single steady state.

Stability of the model inverse is an obvious requirement for the controller in Eq. 20 to be stable. In linear system theory, models with stable inverses are called *minimum phase*. A nonlinear extension of the minimum-phase property is possible using the concept of *zero dynamics* (Isidori, 1989; Kravaris, 1988; Henson and Seborg, 1991). For linear models the zero dynamics are the state-space analog of transfer function zeros (Isidori, 1989). The zero dynamics are usually obtained by transforming the model into *normal form*.

The nonlinear model in Eq. 1 can be transformed into the normal form by a nonlinear change of coordinates. After the application of a suitable, nonlinear, static-state feedback control law, the closed-loop system has the following form in the new coordinates (Isidori, 1989; Kravaris, 1988; Henson and Seborg, 1991):
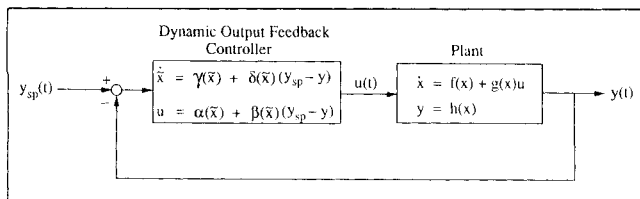
$$\dot{\xi} = A\xi + Bv \qquad (21)$$

$$\dot{\eta} = q(\xi, \eta) \qquad (22)$$

$$\tilde{y} = C\xi \qquad (23)$$

where ξ is a r-dimensional state vector, η is a $(n-r)$-dimensional state vector, v is a new input variable, (A, B, C) are in Brunovsky canonical form, and q is a nonlinear function. The

zero dynamics are obtained by setting the state variables $\xi(t) = 0$ for all $t \geq 0$:

$$\dot{\eta} = q(0, \eta) \qquad (24)$$

Note that the zero dynamics are unobservable from the model output and can affect only the internal stability of the closed-loop system. Stability of the zero dynamics is a necessary condition for a model inverse-based controller to yield an internally stable closed-loop system.

It is tempting to think that this condition is also sufficient because the ξ variables can be forced to zero arbitrarily fast (Byrnes and Isidori, 1985, 1989). In fact, this hypothesis is true if $r = 1$. However, it is not true in general because rapidly decaying ξ variables can induce "peaking" and destroy closed-loop stability (Sussmann, 1990). Hence, a stronger condition is needed to ensure that the closed-loop system will remain stable as the ξ variables decay to zero.

Assumption 5: The nonlinear subsystem in Eq. 22 has the bounded-input bounded-state (BIBS) property with respect to the ξ variables as inputs. If the model satisfies assumption 5, we say the model has a *stable inverse*. The characterization of systems that satisfy the BIBS property is an active area of research (Saberi et al., 1990; Sussmann and Kokotovic, 1991). The IMC strategy proposed in this article is restricted to nonlinear models with stable inverses.

If the model is perfect, Eqs. 16 and 20 yield:

$$y^{(r)}(t) = y_{sp}^{(r)}(t) \qquad (25)$$

If the following initial conditions are satisfied

$$y^{(k)}(0) = y_{sp}^{(k)}(0) \quad 0 \leq k \leq r - 1, \qquad (26)$$

then the model inverse controller provides perfect control as expected:

$$y(t) = y_{sp}(t) \ \forall \ t \geq 0 \qquad (27)$$

Unfortunately, the model inverse controller in Eq. 20 is not suitable for implementation because:

1. Perfect control usually requires unreasonably large control actions.
2. The controller is not "proper" since it differentiates the setpoint.
3. The perfect model assumption is rarely satisfied in practice.
4. The controller is unstable due to pole-zero cancellations at the origin (Kravaris and Kantor, 1990a,b).

The first three problems also occur in linear IMC when the model inverse is used directly as the controller (Morari and Zafiriou, 1989). The fourth problem occurs because the Hirschorn inverse is nonminimal (Kravaris and Kantor, 1990a,b). As shown in the next section, these problems can be avoided by augmenting the model inverse controller with a nonlinear filter.

Figure 2. Proposed structure for nonlinear internal model control.

Filter design

In linear IMC, the model inverse controller is augmented with a filter to obtain an implementable controller. The filter makes the IMC controller proper and provides a tuning parameter that can be adjusted to account for plant/model mismatch. As shown below, the same approach can be used with the nonlinear model inverse controller in Eq. 20 if a nonlinear filter is employed. The filter makes the IMC controller Q proper by eliminating the need for derivatives and contains a single tuning parameter that provides a compromise between performance and robustness. If the model is perfect, input-output stability is guaranteed. When re-arranged into conventional feedback form, the IMC strategy yields a dynamic output feedback control law. Hence, state feedback from the plant is not required.

The nonlinear filter F is chosen to have the following form:

$$v^{(r)} = -\alpha_r L_f^{r-1}\bar{h}(\tilde{x}) - \alpha_{r-1}L_f^{r-2}\bar{h}(\tilde{x})$$
$$- \cdots - \alpha_1\bar{h}(\tilde{x}) + \alpha_1 e \triangleq A(\tilde{x}) + \alpha_1 e \qquad (28)$$

where $v^{(r)}$ is the output of the filter, the $\{\alpha_i\}$ are filter tuning parameters, and the error signal e is defined in Eq. 5. The model inverse controller C is obtained by modifying the input to the controller in Eq. 20:

$$u = -\frac{L_f^r\bar{h}(\tilde{x})}{L_{\tilde{g}}L_f^{r-1}\bar{h}(\tilde{x})} + \frac{1}{L_{\tilde{g}}L_f^{r-1}\bar{h}(\tilde{x})} v^{(r)} \triangleq C(\tilde{x}) + D(\tilde{x})v^{(r)} \qquad (29)$$

The IMC controller $Q = CF$ is obtained by combining Eqs. 28 and 29,

$$u = \frac{\alpha_1 e - \sum_{k=1}^{r+1}\alpha_k L_f^{k-1}\bar{h}(\tilde{x})}{L_{\tilde{g}}L_f^{r-1}\bar{h}(\tilde{x})} \qquad (30)$$

where $\alpha_{r+1} \triangleq 1$. Unlike the model inverse controller in Eq. 20, the IMC controller Q is proper because it does not contain differentiations. The proposed IMC control scheme is shown schematically in Figure 2.

Using Eq. 15, the filter in Eq. 28 can be represented as:

$$v^{(r)} = -\alpha_r\tilde{y}^{(r-1)} - \alpha_{r-1}\tilde{y}^{(r-2)} - \cdots - \alpha_1\tilde{y} + \alpha_1 e \qquad (31)$$

If the following initial conditions are satisfied,

Figure 3. Conventional feedback representation of the proposed nonlinear IMC strategy.

$$\tilde{y}^{(k)}(0) = e^{(k)}(0) \quad 0 \le k \le r - 1, \tag{32}$$

then a closed-loop transfer function (CLTF) between the model output $\tilde{y}$ and the error signal e can be obtained by combining Eqs. 16, 29, and 31:

$$\frac{\tilde{y}(s)}{e(s)} = \frac{\alpha_1}{s^r + \alpha_r s^{r-1} + \cdots + \alpha_2 s + \alpha_1} \tag{33}$$

Note that the condition in Eq. 32 is equivalent to Eq. 26. If the controller parameters $\{\alpha_i\}$ are chosen appropriately (Henson and Seborg, 1990b), the CLTF can be written in terms of a single tuning parameter ϵ:

$$\frac{\tilde{y}(s)}{e(s)} = \frac{1}{(\epsilon s + 1)^r} \tag{34}$$

The filter tuning parameter ϵ can be tuned to provide a compromise between performance and robustness. It is easy to show that no control action is taken in the limit as $\epsilon \to \infty$. As shown in the section on Properties of the Closed-Loop System, the IMC controller Q provides perfect control in the limit as $\epsilon \to 0$. Hence, the filter tuning parameter ϵ has a direct effect on closed-loop performance. The robustness of the proposed IMC strategy will be investigated via simulation study via in the section on the Simulation Study. If assumption 1 holds, Eq. 34 becomes:

$$\frac{y(s)}{y_{sp}(s)} = \frac{1}{(\epsilon s + 1)^r} \tag{35}$$

For a perfect model, the effect of the tuning parameter ϵ on the closed-loop response is particularly simple. Small values of ϵ result in vigorous responses, while large values cause sluggish responses. If $\epsilon > 0$ and y_{sp} is bounded, the plant output is bounded. Hence, the closed-loop system is guaranteed to be input-output stable, if the model is perfect. Internal stability of the closed-loop system will be discussed later.

The CLTF in Eq. 34 can be obtained using the nonlinear IMC method of Economou et al. (1986) if Eq. 29 with $v^{(r)} = e^{(r)}$ is used as the controller and a linear filter F is chosen as:

$$F(s) = \frac{1}{(\epsilon s + 1)^r} \tag{36}$$

Because the linear filter does not affect the stability of the Hirschorn inverse, the resulting IMC controller is unstable (Kravaris and Kantor, 1990a,b). Thus, numerical procedures

based on the contraction mapping principle and Newton's method are required to construct the inverse (Economou and Morari, 1985; Economou et al., 1986). This stability problem does not occur if the nonlinear filter in Eq. 28 is used instead of the linear filter in Eq. 36. As will be shown later, the stability analysis for the nonlinear IMC controller in Eq. 30 is considerably simpler than that required for iterative numerical procedures (Economou and Morari, 1985; Li et al., 1990).

When rearranged into conventional feedback form, the proposed nonlinear IMC strategy yields a dynamic output feedback control law. This can be seen by substituting the filter F in Eq. 28 into the controller C in Eq. 29:

$$u = C(\tilde{x}) + D(\tilde{x})[A(\tilde{x}) + \alpha_1\{y_{sp} - y + \tilde{h}(\tilde{x})\}]$$
$$\triangleq \alpha(\tilde{x}) + \beta(\tilde{x})(y_{sp} - y) \tag{37}$$

Using Eq. 37, the process model in Eq. 1 can be represented as:

$$\dot{\tilde{x}} = \tilde{f}(\tilde{x}) + \tilde{g}(\tilde{x})[\alpha(\tilde{x}) + \beta(\tilde{x})(y_{sp} - y)]$$
$$\triangleq \gamma(\tilde{x}) + \delta(\tilde{x})(y_{sp} - y) \tag{38}$$

Since the controller requires only the plant output y, state feedback from the plant is not required. This important advantage of the proposed approach will be discussed later. The conventional feedback representation of the proposed IMC scheme is shown in Figure 3.

Since the nonlinear filter F in Eq. 28 has proportional action on the error e defined in Eq. 5, large control actions may be generated for step changes in the setpoint. To reduce the size of the control action, an additional setpoint filter may be employed. For example, a filtered setpoint $\tilde{y}_{sp}$ can be obtained from a simple first-order filter with time constant ϵ:

$$\tilde{y}_{sp}(s) = \frac{1}{\epsilon s + 1} y_{sp}(s) \tag{39}$$

Note that the filter in Eq. 39 does not affect closed-loop stability. The error signal e is then defined in terms of $\tilde{y}_{sp}$ instead of y_{sp}. The CLTF for a perfect model in Eq. 35 becomes:

$$\frac{y(s)}{y_{sp}(s)} = \frac{1}{(\epsilon s + 1)^{r+1}} \tag{40}$$

Application to a linear process model

In this section, the proposed nonlinear IMC strategy is applied to a linear process model to compare it with the linear IMC design method. As in the nonlinear case, the SISO model is assumed to be open-loop stable and minimum phase. An IMC controller is first designed for a transfer function model using the standard approach of Morari and Zafiriou (1989). The proposed IMC strategy is then applied to a state-space realization of the transfer function model. The model inverse controllers and filters obtained using the transfer function and state-space methods are identical. Hence, for open-loop stable, minimum-phase linear systems, the two approaches are equiv-

alent. Unlike the transfer function approach, the proposed state-space strategy generalizes readily to nonlinear systems.

Consider the following SISO transfer function model:

$$\frac{\tilde{y}(s)}{u(s)} = \tilde{G}(s) = \tilde{K}\frac{s^{n-r} + \tilde{b}_{n-r-1}s^{n-r-1} + \cdots + \tilde{b}_1 s + \tilde{b}_0}{s^n + \tilde{a}_{n-1}s^{n-1} + \cdots + \tilde{a}_1 s + \tilde{a}_0}$$

$$\triangleq \tilde{K}\frac{\tilde{b}(s)}{\tilde{a}(s)} \quad (41)$$

The polynomials $\tilde{a}(s)$ and $\tilde{b}(s)$ are Hurwitz by assumption. Note that the relative degree r is the difference between the orders of the denominator and numerator polynomials and $r \geq 0$ if $\tilde{G}(s)$ is proper. Because the model is open-loop stable and minimum phase, the model inverse controller is chosen as (Morari and Zafiriou, 1989):

$$\frac{u(s)}{v(s)} = C(s) = \tilde{G}^{-1}(s) = \frac{1}{\tilde{K}}\frac{\tilde{a}(s)}{\tilde{b}(s)} \quad (42)$$

Note that $C(s)$ is improper if $r > 0$. An implementable controller is obtained by augmenting $C(s)$ with an rth-order linear filter,

$$F(s) = \frac{1}{(\epsilon s + 1)^r} \quad (43)$$

where ϵ is the filter tuning parameter. The IMC controller $Q(s)$ is obtained by combining $C(s)$ and $F(s)$ as in Eq. 3:

$$Q(s) = \frac{1}{\tilde{K}}\frac{\tilde{a}(s)}{\tilde{b}(s)}\frac{1}{(\epsilon s + 1)^r} \quad (44)$$

To apply the proposed IMC strategy, a linear state-space model is required,

$$\dot{\tilde{x}} = \tilde{A}\tilde{x} + \tilde{B}u \quad (45)$$
$$\tilde{y} = \tilde{C}\tilde{x}$$

where $\tilde{x}$ is an n-dimensional state vector, $\tilde{A}$ is an $n \times n$ matrix, $\tilde{B}$ is a $n \times 1$ column vector, and $\tilde{C}$ is a $1 \times n$ row vector. Unlike the nonlinear model in Eq. 1, the linear model in Eq. 45 cannot have singular points. Hence, assumption 3 is not required and the relative degree in Eqs. 13 and 14 is defined as:

$$r \triangleq \min\{k: \ \tilde{C}\tilde{A}^{k-1}\tilde{B} \neq 0\} \quad (46)$$

Hence, the first r time derivatives of the model output in Eqs. 15 and 16 can be written as:

$$\tilde{y}^{(k)} = \tilde{C}\tilde{A}^k\tilde{x} \quad 1 \leq k \leq r - 1 \quad (47)$$

$$\tilde{y}^{(r)} = \tilde{C}\tilde{A}^r\tilde{x} + \tilde{C}\tilde{A}^{r-1}\tilde{B}u \quad (48)$$

It follows from Eqs. 47 and 48 that the filter F in Eq. 28 and model inverse controller C in Eq. 29 are:

$$v^{(r)} = -\alpha_r\tilde{C}\tilde{A}^{r-1}\tilde{x} - \alpha_{r-1}\tilde{C}\tilde{A}^{r-2}\tilde{x} - \cdots - \alpha_1\tilde{C}\tilde{x} + \alpha_1 e \quad (49)$$

$$u = -\frac{\tilde{C}\tilde{A}^r}{\tilde{C}\tilde{A}^{r-1}\tilde{B}}\tilde{x} + \frac{1}{\tilde{C}\tilde{A}^{r-1}\tilde{B}}v^{(r)} \quad (50)$$

The IMC controller Q in Eq. 30 is obtained by combining Eqs. 49 and 50,

$$u = \frac{\alpha_1 e - \sum_{k=1}^{r+1}\alpha_k\tilde{C}\tilde{A}^{k-1}\tilde{x}}{\tilde{C}\tilde{A}^{r-1}\tilde{B}} \quad (51)$$

where $\alpha_{r+1} \triangleq 1$.

If the proposed IMC strategy is applied to a state-space realization of the transfer function in Eq. 41, the IMC controllers in Eqs. 44 and 51 can be directly compared. It can be shown that the zero dynamics represent the dynamics of the inverse system (Isidori, 1989). Moreover, the IMC controllers obtained using the transfer function and state-space approaches are equivalent.

Theorem 1: If the transfer function model in Eq. 41 is open-loop stable and minimum phase, and the IMC controllers in Eqs. 44 and 51 have identical input-output behavior. The proof of theorem 1 is in the Appendix. Hence, the transfer function and state-space approaches are equivalent for open-loop stable, minimum-phase linear systems. As shown in the previous sections, the proposed state-space strategy readily generalizes to nonlinear systems.

Properties of the closed-loop system

Economou et al. (1986) have shown that the general nonlinear IMC structure in Figure 1 possesses the same stability, perfect control, and zero offset properties as linear IMC (Morari and Zafiriou, 1989). In this section, we show that under suitable assumptions the closed-loop system in Figure 2 satisfies analogous properties. The proofs of the four theorems presented below are in the Appendix.

Theorem 2: If $\epsilon = 0$, assumptions 2 and 3 hold, the condition in Eq. 26 is satisfied, and the plant and models outputs are bounded, then the IMC controller in Eq. 30 is a model inverse controller and perfect control is obtained. Since the controller takes no control action in the limit as $\epsilon \to \infty$, theorem 2 shows that the filter tuning parameter ϵ has a direct effect on the closed-loop performance. Additionally, the proof of theorem 2 shows that the nonlinear filter in Eq. 28 reduces to $v^{(r)} = e^{(r)}$ when $\epsilon = 0$. Thus, the filter provides the controller C in Eq. 29 with an "approximate" value of $e^{(r)}$ when $\epsilon > 0$. In this sense, an improper model inverse controller can be approximated to any degree of accuracy by the proper controller in Eq. 30 by reducing the filter parameter ϵ.

Theorem 3: If assumptions 1–3 and assumption 5 are satisfied, y_{sp} is bounded, and $\epsilon > 0$, then the IMC controller in Eq. 30 yields a closed-loop system that is internally stable and input-output stable. As discussed earlier, the zero dynamics must satisfy the BIBS property in assumption 5 to ensure that the closed-loop system is internally stable.

Theorem 4: If the closed-loop system is asymptotically stable, then the IMC controller in Eq. 30 eliminates offset. Note

Table 1 Nonlinear IMC vs. Exact I/O Linearizing Control

Comparison	Nonlinear IMC	Exact I/O Linearization
Model Runs in Parallel?	Yes	No
Need Plant State?	No	Yes
Controller Type	Dynamic output FB	Static state FB
Integral Action	Implicit	Explicit
CLTF if $M \neq P$	$\dfrac{\bar{y}(s)}{e(s)} = \dfrac{1}{(\epsilon s + 1)^r}$	None
Perfect Control if $Q = M_r^{-1}$?	Yes	No
Limitations	Open-loop stable systems with stable inverses	Systems with stable inverses

that the asympotic stability assumption implies that the set-point and any disturbances are asymptotically constant.

Theorem 5: If assumption 1 with $\tilde{x}(0) \neq x(0)$ is satisfied, assumption 4 is satisfied, and $u(t) = u_o$ for all $t \geq 0$, then the model state converges asymptotically to the plant state. Note that theorem 5 requires that u is a constant (there is no feedback control). This assumption cannot be avoided since there is no general separation property for nonlinear systems (Isidori, 1989). The proof of the theorem indicates that the state estimation error converges according to the open-loop dynamics of the process. This property and the open-loop stability requirement are the major disadvantages of a nonlinear open-loop observer.

Comparison with input-output linearization

Several controller design techniques based on exact input-output linearization have recently been developed for nonlinear process control (Kravaris and Chung, 1987; Lee and Sullivan, 1988; Bartusiak et al., 1989; Henson and Seborg, 1990b). In this section, the proposed nonlinear IMC strategy is compared to input-output linearizing control. The IMC controller can be interpreted as the combination of an input-output linearizing controller and an open-loop observer. Thus, an important advantage of the IMC approach is that full-state feedback is not required. The IMC strategy is also compared to input-output linearizing control strategies that employ open-loop observers.

An input-output linearizing controller can be designed to have the form (Kravaris and Kantor, 1990b; Henson and Seborg, 1991),

$$u = \frac{\alpha_0 \displaystyle\int_0^t (y_{sp} - y)\,dt - \sum_{k=1}^{r+1} \alpha_k L_f^{k-1} \tilde{h}(x)}{L_g L_f^{r-1} \tilde{h}(x)} \tag{52}$$

where the $\{\alpha_i\}$ are tuning parameters and $\alpha_{r+1} \triangleq 1$. If the model is perfect, the $\{\alpha_i\}$ can be chosen to yield the following CLTF (Henson and Seborg, 1990b; Kravaris and Kantor, 1990b):

$$\frac{y(s)}{y_{sp}(s)} = \frac{1}{(\epsilon s + 1)^{r+1}} \tag{53}$$

Note that Eqs. 52 and 53 are similar to the IMC controller Q

and CLTF in Eqs. 30 and 35, respectively. However, there are several important differences between the two techniques. Most importantly, the linearizing controller in Eq. 52 requires full state feedback from the plant. Conversely, the IMC controller only requires the plant output since the model functions as an open-loop observer. Hence, the IMC controller can be interpreted as the combination of an input-output linearizing controller and an open-loop observer. As shown in Figure 3, the IMC strategy yields a dynamic output feedback controller. The input-output linearization approach produces a static-state feedback controller (Kravaris and Kantor, 1990b; Henson and Seborg, 1991).

The IMC approach implicitly includes integral action by using the difference between the plant and model outputs as a feedback signal. Conversely, an integral term must be added to the linearizing control law to ensure offset-free performance. As shown in Eq. 53, the integral term increases the relative degree of the closed-loop system. This can adversely affect the disturbance rejection properties of the nonlinear controller (Henson and Seborg, 1990b). Note that the CLTF in Eq. 53 was derived under the assumption of a perfect model. In contrast to nonlinear IMC, a CLTF cannot be obtained for the input-output linearization approach if the model is imperfect. As shown in the proof of theorem 2, the CLTF in Eq. 34 is essential in proving that the IMC strategy can provide perfect control even if the model is imperfect.

Both techniques require assumptions 1–3 and assumption 5 to ensure closed-loop stability. As shown in theorem 5, a disadvantage of the IMC approach is that open-loop unstable systems cannot be addressed. If nonlinear closed-loop observers are employed in the IMC strategy, assumption 4 can be removed. Unfortunately, closed-loop observers can be designed for only a very limited class of nonlinear systems (Isidori, 1989; Kantor, 1989). The comparison of the nonlinear IMC and input-output linearization techniques is summarized in Table 1.

Dynamic output feedback controllers have also been designed by combining nonlinear open-loop observers and input-output linearizing controllers (Kravaris and Chung, 1987; Daoutidis and Kravaris, 1991). For open-loop stable systems, the controller design is based on the Hirschorn inverse, while a minimal inverse is employed for open-loop unstable systems. Although the control scheme can be interpreted from an IMC perspective, the IMC structure in Figure 1 is not used for controller design. Hence, the input-output linearization strategy does not enjoy many of the beneficial features, such as the perfect control property, of the proposed nonlinear IMC approach. Moreover, the controller proposed for open-loop, unstable systems usually contains derivatives of the output that may be problematic if the output is corrupted with high-frequency noise. The stability and performance of the input-output linearization strategy has been analyzed only when the model is perfect and the open-loop observer is perfectly initialized. Under these conditions, the plant and model are identical. Finally, limited simulation results for the input-output linearization scheme have been presented.

Extensions for nonlinear systems with measured disturbances

In this section, the nonlinear IMC strategy is extended to
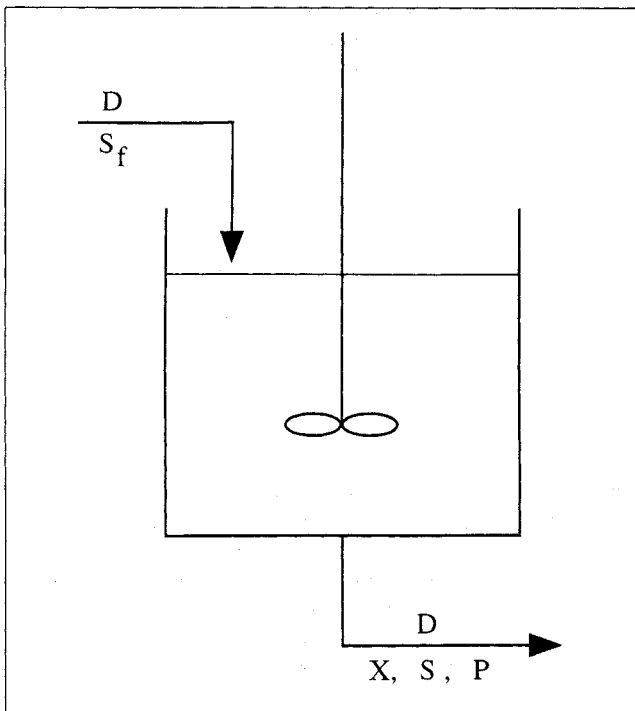
Figure 4. Continuous fermentor.

nonlinear systems with measured disturbances. Assume that the SISO model M available for controller design has the form,

$$\dot{\tilde{x}} = \tilde{f}(\tilde{x}) + \tilde{g}(\tilde{x})u + \tilde{p}(\tilde{x})\tilde{d} \tag{54}$$
$$\tilde{y} = \tilde{h}(\tilde{x})$$

where $\tilde{d}$ is a $\tilde{q}$-dimensional vector of disturbances and $\tilde{p}$ is a $n \times \tilde{q}$ matrix of nonlinear functions. The plant P is assumed to have the form:

$$\dot{x} = f(x) + g(x)u + p(x)d \tag{55}$$
$$y = h(x)$$

where d is a q-dimensional vector of disturbances and p is a $n \times q$ matrix of nonlinear functions. If the ith disturbance is measured, $\tilde{d}_i(t) = d_i(t)$. The controller design strategy can be extended to models in which u and/or $\tilde{d}$ appear nonlinearly (Henson and Seborg, 1990b).

As in the disturbance-free case, the nominal performance criterion in Eq. 4 is minimized if the controller C is the right inverse of the model as in Eq. 9. However, the construction of the inverse is more complex than in the disturbance-free case. In analogy to Eqs. 13 and 14, the ith disturbance in Eq. 54 is said to have *relative degree* ρ_i at a point $\tilde{x}_o$ if:

(i) $\quad L_{\tilde{p}_i} L_{\tilde{f}}^{k-1} \tilde{h}(\tilde{x}) = 0$

$\quad \forall\ x$ in a neighborhood of $\tilde{x}_o$ and $\forall\ k < \rho_i - 1$ (56)

(ii) $\quad L_{\tilde{p}_i} L_{\tilde{f}}^{\rho_i - 1} \tilde{h}(\tilde{x}_o) \neq 0$ (57)

The relative effects of the manipulated input and disturbances on the model output can be characterized be defining the fol-

lowing classes of disturbances (Daoutidis and Kravaris, 1989):

$$\tilde{d}_{\textcircled{A}} \triangleq \{\tilde{d}_i:\ \rho_i > r\}$$
$$\tilde{d}_{\textcircled{B}} \triangleq \{\tilde{d}_i:\ \rho_i = r\} \tag{58}$$
$$\tilde{d}_{\textcircled{C}} \triangleq \{\tilde{d}_i:\ \rho_i < r\}$$

The $\tilde{d}_{\textcircled{A}}$ and $\tilde{d}_{\textcircled{B}}$ disturbances pose no difficulties in the construction of the model inverse. However, the $\tilde{d}_{\textcircled{C}}$ disturbances are problematic because they affect the output more directly than u. If the model contains $\tilde{d}_{\textcircled{C}}$ disturbances, the model inverse contains time derivatives of the disturbances (Daoutidis and Kravaris, 1989). To avoid such derivatives in the IMC control law, we assume that there are no $\tilde{d}_{\textcircled{C}}$ disturbances.

Assumption 6: $\tilde{d}_{\textcircled{C}} = \{0\}$. If assumption 6 is not satisfied, derivatives in the control law can be avoided by using nominal values for the $\tilde{d}_{\textcircled{C}}$ disturbances.

In analogy to the disturbance-free case, the filter is chosen as in Eq. 28 and the controller C is:

$$u = -\frac{L_{\tilde{f}}^r \tilde{h}(\tilde{x})}{L_{\tilde{g}} L_{\tilde{f}}^{r-1} \tilde{h}(\tilde{x})} + \frac{1}{L_{\tilde{g}} L_{\tilde{f}}^{r-1} \tilde{h}(\tilde{X})} v^{(r)}$$
$$-\frac{\sum\limits_{\tilde{d}_i \in d_{\textcircled{B}}} L_{\tilde{p}_i} L_{\tilde{f}}^{r-1} \tilde{h}(\tilde{x}) \tilde{d}_i}{L_{\tilde{g}} L_{\tilde{f}}^{r-1} \tilde{h}(\tilde{x})} \tag{59}$$

Note that the $\tilde{d}_{\textcircled{A}}$ disturbances can be incorporated in the model in Eq. 54, while the $\tilde{d}_{\textcircled{B}}$ disturbances can be used in the model and controller C in Eq. 59. If the initial conditions in Eq. 26 are satisfied, the IMC controller Q in Eqs. 28 and 59 yields the CLTF in Eq. 34. As in the disturbance-free case, the filter parameter ϵ can be tuned to provide a compromise between performance and robustness. If assumptions 1–5 are modified to account for the disturbances in Eq. 54, the closed-loop system satisfies the properties in a previous section. The nonlinear IMC controller in Eqs. 28 and 59 is closely related to so-called *disturbance decoupling* control laws (Hirschorn, 1981; Isidori et al., 1981; Daoutidis and Kravaris, 1989; Henson and Seborg, 1990b). In fact, the IMC control law can be interpreted as the combination of a disturbance decoupling controller and a nonlinear open-loop observer.
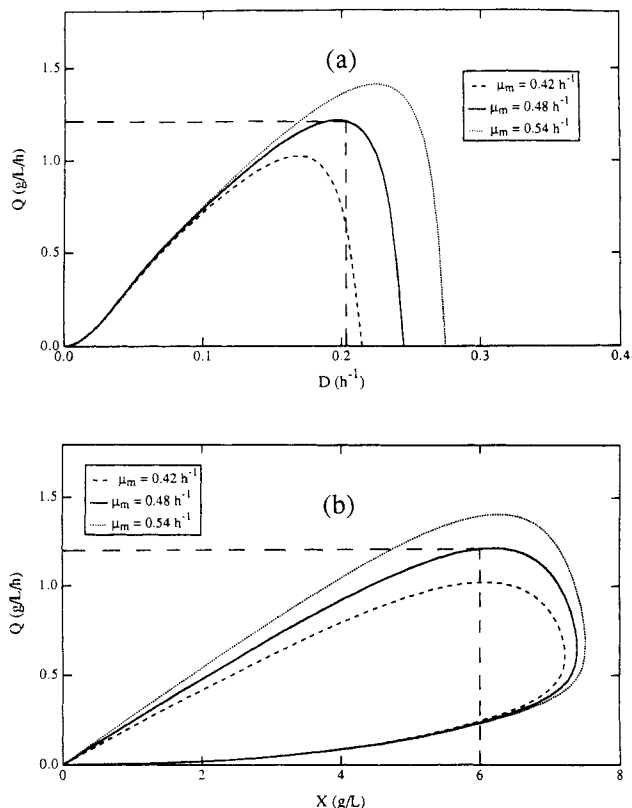
Simulation Study

In this section, the proposed nonlinear IMC strategy is applied to a continuous fermentor. The IMC approach is compared to a conventional PI controller and an input-output linearizing controller based on full state feedback. A schematic of a constant volume fermentor is shown in Figure 4. The dilution rate D and the feed substrate concentration S_f are process inputs. The dilution rate is usually selected as the manipulated variable. If the effluent cell (biomass) concentration X, substrate concentration S, and product concentration P are chosen as process state variables, the fermentor is described by three nonlinear ordinary differential equations (Agrawal et al., 1989),

$$\dot{X} = -DX + \mu X \tag{60}$$

Figure 5. Effect of (a) the dilution rate and (b) the cell concentration on the productivity for three μ_m values.

$$\dot{S} = D(S_f - S) - \frac{1}{Y_{x/s}}\mu X \qquad (61)$$

$$\dot{P} = -DP + (\alpha\mu + \beta)X \qquad (62)$$

where μ is the specific growth rate, $Y_{x/s}$ is the cell-mass yield, and α and β are kinetic parameters. The specific growth rate may exhibit both substrate and product inhibition,

$$\mu = \frac{\mu_m\left(1 - \dfrac{P}{P_m}\right)S}{K_m + S + \dfrac{S^2}{K_i}} \qquad (63)$$

where Eq. 63 contains four parameters: the maximum specific growth rate μ_m, the product saturation constant P_m, the substrate saturation constant K_m, and the substrate inhibition constant K_i. For many fermentations, the maximum specific growth rate μ_m and cell-mass yield $Y_{x/s}$ exhibit significant time-varying behavior and can, therefore, be viewed as unmeasured disturbances (Henson and Seborg, 1990a).

For most continuous fermentations, the control objective is to maximize the steady-state productivity $\overline{Q}$. If the biomass is the desired product, $\overline{Q}$ can be defined as the amount of biomass produced per unit time,

$$\overline{Q} = \overline{DX} \qquad (64)$$

Table 2 Nominal Fermentor Parameters and Operating Conditions

Variable	Nominal Value
$Y_{x/s}$	0.4 g/g
α	2.2 g/g
β	0.2 h^{-1}
μ_m	0.48 h^{-1}
P_m	50 g/L
K_m	1.2 g/L
K_i	22 g/L
S_f	20 g/L
D	0.202 h^{-1}
X	6.0 g/L
S	5.0 g/L
P	19.14 g/L

where the overbar represents a steady-state value. As shown in Figure 5a, small μ_m disturbances may have a dramatic effect on the optimum productivity. Moreover, the dilution rate required to obtain the optimum productivity also varies significantly with μ_m. Conversely, Figure 5b demonstrates that the cell concentration X corresponding to the optimum productivity is essentially constant despite changes in μ_m. Similar behavior for $Y_{x/s}$ indicates that near optimal productivity can be achieved by regulating X at a constant value.

Since the cell concentration often can be measured or estimated (Johnson, 1987), the biomass X is a reasonable choice for the controlled output. Although direct productivity control is possible (Henson and Seborg, 1990a), Figure 5a indicates that the productivity setpoint must be carefully chosen to ensure that it is near-optimal and feasible. Nominal parameters and operating conditions (Agrawal et al., 1989) used for the simulations are listed in Table 2 and indicated by the dashed lines in Figure 5. The open-loop responses shown in Figure 6 indicate that the fermentor exhibits significant static and dynamic nonlinear behavior in the region of operation. If the state variables, manipulated input, disturbance, and controlled output are defined as

$$x \triangleq [X\ S\ P]^T,\ u \triangleq D,\ d \triangleq \mu_m\ \text{or}\ d \triangleq Y_{x/s},\ y \triangleq X, \qquad (65)$$

the process P can be represented by Eq. 55. The model M in Eq. 54 used for controller design may differ from P in a variety of ways. For instance, the specific growth rate μ of the model can be a simple Monod expression (Agrawal et al., 1989; Johnson, 1987) instead of Eq. 63. Several types of modeling error are considered in the simulations.

The fermentation model satisfies most of the assumptions described earlier. The smoothness and regularity conditions in assumptions 2 and 3 are satisfied in the desired region of operation. Simulation results indicate that the zero dynamics satisfy the BIBS property in assumption 5. Since the relative degree of input $r = 1$, the matching condition in assumption 6 is trivially satisfied. The model, however, can exhibit multiple steady states (Henson and Seborg, 1990a), so the open-loop stability condition in assumption 4 is not always satisfied. Moreover, for most of simulations presented below, the perfect model condition in assumption 1 does not hold. Despite these difficulties, the nonlinear internal model controller can be designed as described earlier.

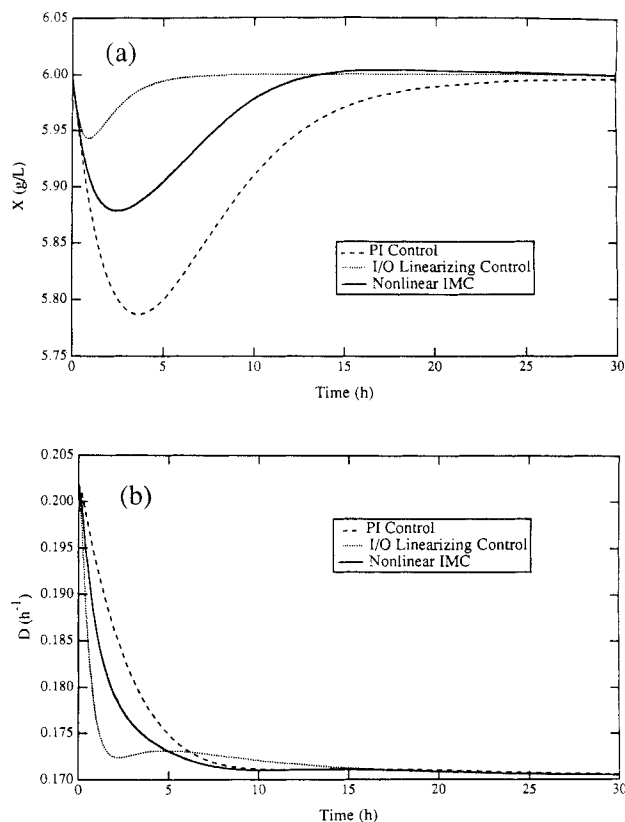For comparison, three controllers were designed: a conven-
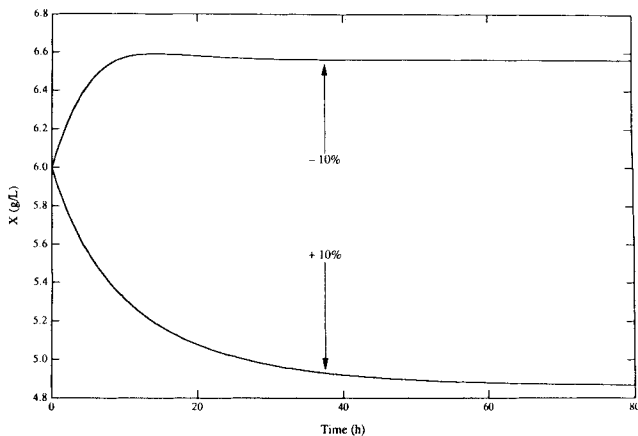
Figure 6. Open-loop cell concentration responses for step changes in the dilution rate.

Figure 8. μ_m **disturbance: (a) cell concentration and (b) dilution rate.**

tional PI controller, an input-output (I/O) linearizing controller based on full state feedback, and a nonlinear internal model controller (NIMC) controller. The PI controller parameters were initially determined using internal model control tuning rules (Morari and Zafiriou, 1989) for two first-order models obtained from the responses in Figure 6. In each case, the IMC closed-loop time constant τ_c was chosen to be one-third the open-loop time constant. The parameters were then fine-tuned to provide a compromise between the two setpoint responses in Figure 7a. The resulting PI controller parameters $K_c = -0.07$ L/g·h and $\tau_I = 4.5$ h were used in all simulations.
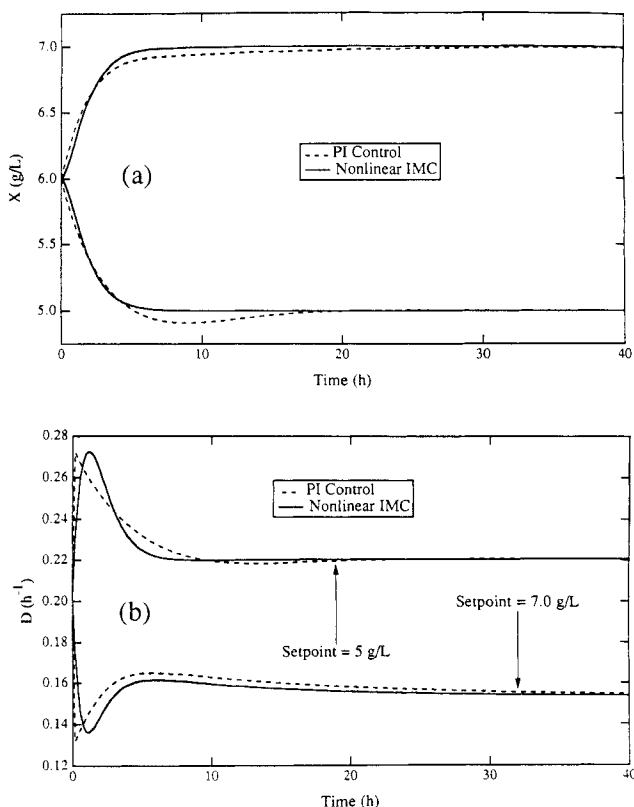
Figure 7. Step changes in the setpoint: (a) cell concentration and (b) dilution rate.

Because the disturbances in Eq. 65 are assumed to be unmeasurable, the I/O linearizing controller has the form in Eq. 52, while the IMC controller has the form in Eqs. 28 and 29. For both nonlinear controllers, the closed-loop time constant $\epsilon = 1$ h was used in all simulations. This value is about one-third the open-loop time constant for the -10% dilution rate change in Figure 6.

Setpoint responses for the PI controller and NIMC are shown in Figure 7a. In this case, the I/O linearizing controller is equivalent to the NIMC since the model is assumed to be perfect. The performance of the PI controller and NIMC is very similar. Figure 7b shows that the two controllers require about the same amount of control action to accomplish the setpoint changes. Hence, the controllers have been tuned to provide equal setpoint responses. In subsequent simulations, the disturbance rejection capabilities of the three controllers will be analyzed using the tuning parameters determined for the setpoint changes in Figure 7.

In Figure 8, the three controllers are compared for an unmeasured step disturbance of -12.5% in the maximum growth rate μ_m occurring at $t = 0$. Since $\rho = 1$ and the disturbance cannot be measured, the I/O linearizing controller cannot decouple the disturbance from the output. However, Figure 8a indicates that the I/O linearizing controller provides the best disturbance rejection since it uses all three state variables. For the PI controller and NIMC that require only the plant output X, the NIMC is clearly superior. The control moves shown in Figure 8b are similar for the three controllers.

In Figure 9a, the three controllers are compared for a -20%
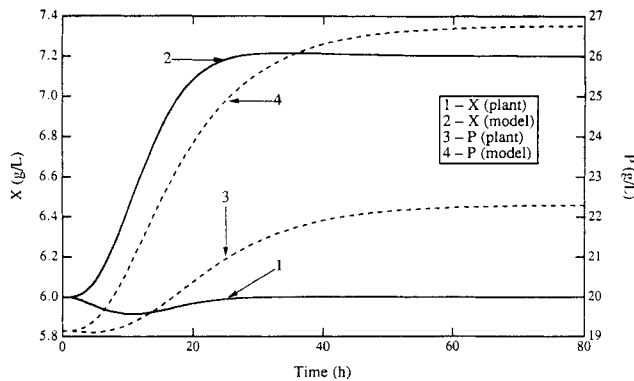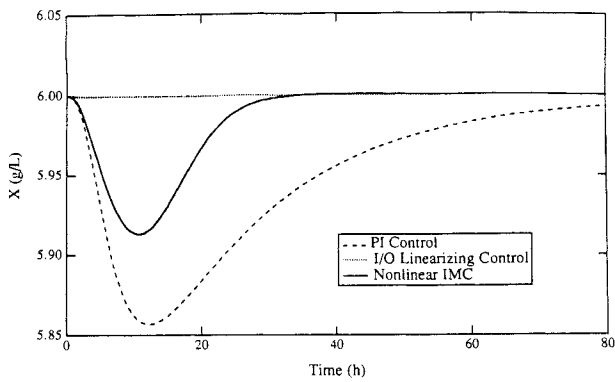
Figure 9. $Y_{x/s}$ disturbance: (a) cell concentration and (b) IMC state estimates.

step disturbance in the cell-mass yield $Y_{x/s}$ occurring at $t = 0$. Since $r = 1$, the model is perfect (except for the disturbance), and $\rho = 2$ for this disturbance, the I/O linearizing controller provides perfect disturbance decoupling. Conversely, the NIMC cannot decouple the disturbance from the output since it uses the state estimates from the model. However, the NIMC rejects the disturbance much better than does the PI controller. In Figure 9b, the actual and estimated values of X and P are shown. Despite the significant errors in the X and P estimates,
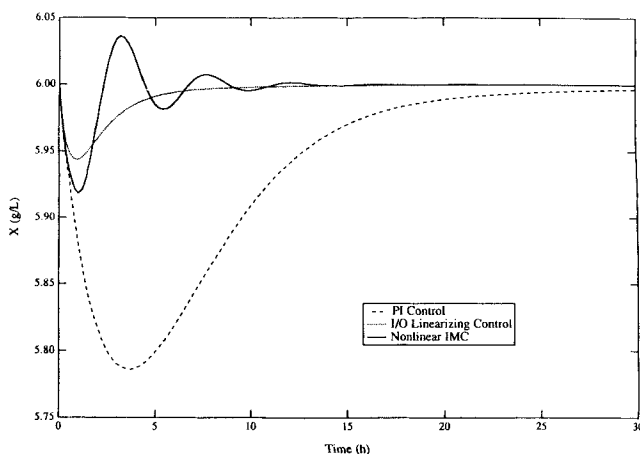
Figure 10. Cell concentration responses for a μ_m disturbance when the model contains an error in the growth rate expression.
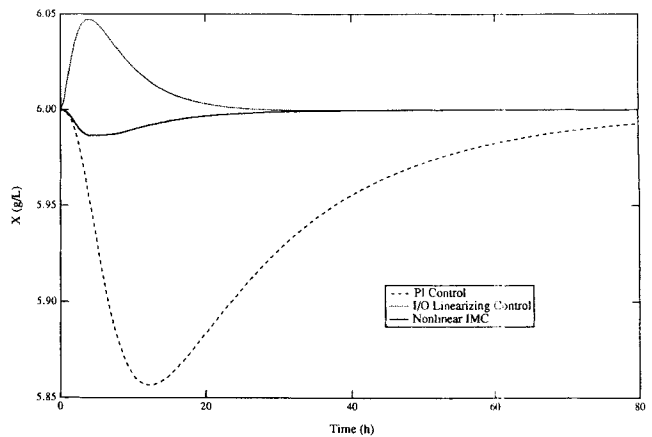
Figure 11. Cell concentration responses for a $Y_{x/s}$ disturbance when the model contains an error in the growth rate expression.

the NIMC is able to provide excellent control. Note that the NIMC rejects the $Y_{x/s}$ disturbance slightly better than the μ_m disturbance. This is expected since ρ is larger for the $Y_{x/s}$ disturbance (Henson and Seborg, 1990a).

Figures 10 and 11 show the performance of the three controllers for the same disturbances in Figures 8 and 9, respectively, except that the model contains a structural error in the growth rate:

$$\mu = \frac{\mu_m S}{K_m + S} \tag{66}$$

The Monod expression in Eq. 66 can be obtained from Eq. 63 by setting $P_m = \infty$ and $K_i = \infty$. Since this modeling error does not affect the process, the PI controller responses do not change from Figures 8a and 9a. For the μ_m disturbance in Figure 10, the I/O linearizing controller provides the best disturbance rejection. Although the NIMC response is oscillatory, it is superior to that of the PI controller. Somewhat surprisingly, the NIMC outperforms the I/O linearizing controller for the $Y_{x/s}$ disturbance in Figure 11. In fact, the NIMC response is much better than that in Figure 9a when no modeling error (except for the disturbance) is present. This example indicates that the disturbance decoupling property of the I/O linearizing controller is not always important since it requires a perfect model. These two disturbances indicate that the NIMC is quite robust to structural modeling errors.

To further evaluate the NIMC, the model was simplified so that the process contained unmodeled dynamics. Existing robustness theory for nonlinear process control (Kravaris and Palanki, 1988) cannot address this type of plant/model mismatch. In particular, the model was simplified using slow manifold theory (Marino and Kokotovic, 1988). If a system starts on a manifold and evolves on that manifold for a certain period of time, the manifold is said to be *invariant* to the flow of the system. It is easy to show that if the fermentor is initially as steady state and $\beta = 0$,

$$P - \alpha X = 0 \tag{67}$$

is an invariant manifold. Because $\beta = 0.2 \text{ h}^{-1}$, the manifold in
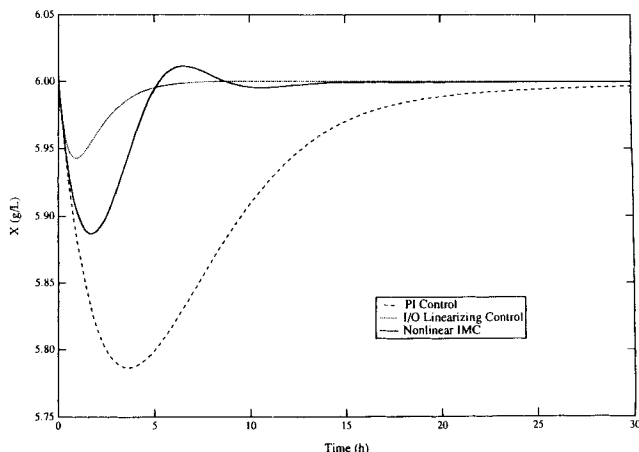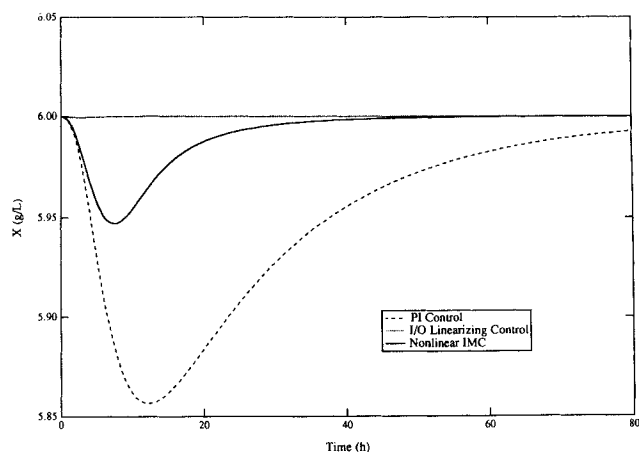
Figure 12. Cell concentration responses for a μ_m disturbance when only the cell concentration dynamics are modeled.

Eq. 67 is not actually invariant. However, slow manifold theory indicates that the fermentor converges "quickly" to a manifold "near" Eq. 67. Hence, the condition in Eq. 67 holds in an approximate sense when β is nonzero, but small. If the fermentor is initially at steady state and $Y_{x/s}$ is constant,

$$S_f - S - \frac{1}{Y_{x/s}} X = 0 \tag{68}$$

is also an invariant manifold. If the $Y_{x/s}$ disturbances are small, the condition in Eq. 68 holds in an approximate sense. The model used to design the NIMC was Eqs. 60 and 63 where the estimates of P and S were obtained from the algebraic equations in Eqs. 67 and 68, respectively.

The NIMC based on the reduced-order model was evaluated for the same disturbances used in Figures 8a and 9a. The results for the μ_m disturbance are shown in Figure 12 along with responses of the PI and I/O linearizing controllers in Figure 8a. Since the process is unchanged and the I/O linearizing controller is based on full-scale feedback, the responses of

Figure 13. Cell concentration responses for a $Y_{x/s}$ disturbance when only the cell concentration dynamics are modeled.

these two controllers are not changed by the unmodeled dynamics. Although the NIMC response is slightly oscillatory, it is still superior to the PI controller response. In fact, the NIMC is comparable to the I/O linearizing controller based on full-state feedback. The three controllers are compared for the $Y_{x/s}$ disturbance in Figure 13. As in Figure 8a, the I/O linearizing controller perfectly decouples the output and the disturbance. Despite the unmodeled dynamics, the NIMC is clearly superior to the PI controller. These results indicate that the NIMC is robust to unmodeled dynamics. The simulation results demonstrate that the NIMC is able to provide excellent control if significant modeling errors are present.

Conclusions

An internal model control strategy has been developed for nonlinear single-input single-output systems. Unlike other nonlinear control techniques that incorporate IMC concepts, the proposed approach is a general extension of linear IMC to open-loop, stable, nonlinear systems with stable inverses. The controller is based on the inverse of the process model and a nonlinear filter is added to make the controller implementable and to account for modeling errors. An important advantage of the new approach is that the assumption of full-state feedback inherent in most input-output linearization schemes is eliminated. Under reasonably mild assumptions, the closed-loop system possesses the same stability, perfect-control, and zero-offset properties as linear IMC. A linear process model was used to compare the new approach to linear IMC, and extensions for nonlinear systems with disturbances were proposed. Simulation results for a continuous fermentor demonstrate that the nonlinear IMC strategy is superior to conventional PI control and compares favorably to input-output linearizing control based on full-state feedback.

Notation

a = denominator polynomial of transfer function
b = numerator polynomial of transfer function
C = controller
d = disturbance vector
D = dilution rate
e = error signal
f, g = vector fields
G = transfer function
h = output function
K = steady-state gain
K_i = substrate inhibition constant
K_m = substrate saturation constant
$L_f^k h$ = kth order Lie derivative of h with respect to f
M_r^{-1} = right inverse of the process model
P = product concentration
Q = productivity
P_m = product saturation constant
r = relative degree of the manipulated input
S = substrate concentration
S_f = feed substrate concentration
t = time
u = manipulated input
v = output of the filter
x = state vector
X = cell concentration
y = controlled output
y_{sp} = setpoint

$\bar{y}_{sp}$ = filtered setpoint
$Y_{x/s}$ = cell-mass yield

Greek letters

α, β = kinetic parameters for fermentor
α_i = controller tuning parameters
ϵ = filter time constant
η, ξ = transformed state variables
ρ_i = relative degree of the ith disturbance
μ = growth rate
μ_m = maximum growth rate

Subscripts

o = constant value

Superscripts

$\sim$ = model
$-$ = steady-state value

Literature Cited

Agrawal, P., G. Koshy, and M. Ramseier, "An Algorithm for Operating a Fed-Batch Fermentor at Optimum Specific-Growth Rate," *Biotech. Bioeng.*, **33**, 115 (1989).

Alvarez-Gallegos, J., and J. Alvarez-Gallegos, "Tracking and Regulation Reference Model Control of Nonlinear Systems," IFAC Symp. on Nonlinear Control Systems Design, Capri, Italy, 466 (1989).

Bartee, J. F., K. F. Bloss, and C. Georgakis, "Design of Nonlinear Reference System Control Structures," AIChE Meeting, San Francisco (1989).

Bartusiak, R. D., C. Georgakis, and M. J. Reilly, "Nonlinear Feedforward/Feedback Control Structures Designed by Reference System Synthesis," *Chem. Eng. Sci.*, **44**, 1837 (1989).

Boothby, W. M., *An Introduction to Differentiable Manifolds and Riemannian Geometry*, 2nd ed., Academic Press, New York (1986).

Byrnes, C. I., and A. Isidori, "Global Feedback Stabilization of Nonlinear Systems," *Proc. IEEE Conf. on Decision and Control*, Ft. Lauderdale, 1031 (1985).

Byrnes, C. I., and A. Isidori, "New Results and Examples in Nonlinear Feedback Stabilization," *Sys. and Cont. Lett.*, **12**, 437 (1989).

Calvet, J., and Y. Arkun, "Feedforward and Feedback Linearization of Nonlinear Systems and Its Implementation Using Internal Model Control (IMC)," *Ind. Eng. Chem. Res.*, **27**, 1822 (1988).

Daoutidis, P., and C. Kravaris, "Synthesis of Feedforward/Feedback Controllers for Nonlinear Processes," *AIChE J.*, **35**, 1602 (1989).

Daoutidis, P., and C. Kravaris, "Dynamic Output Feedback Control of Minimum-Phase Nonlinear Processes," *Chem. Eng. Sci.*, in press (1991).

DiBiasio, D., H. C. Lim, and W. A. Weigand, "An Experimental Investigation of Stability and Multiplicity of Steady States in a Biological Reactor," *AIChE J.*, **27**, 284 (1981).

Economou, C. G., and M. Morari, "Newton Control Laws for Nonlinear Controller Design," *Proc. IEEE Conf. on Decision and Control*, Ft. Lauderdale, 1361 (1985).

Economou, C. G., M. Morari, and B. O. Palsson, "Internal Model Control. 5. Extension to Nonlinear Systems," *Ind. Eng. Chem. Proc. Des. and Dev.*, **25**, 403 (1986).

Henson, M. A., and D. E. Seborg, "Nonlinear Control Strategies for Continuous Fermentors," *Proc. Amer. Control. Conf.*, San Diego, 2723 (1990a).

Henson, M. A., and D. E. Seborg, "Input-Output Linearization of General Nonlinear Processes," *AIChE J.*, **36**, 1753 (1990b).

Henson, M. A., and D. E. Seborg, "A Critique of Exact Linearization Strategies for Process Control," *J. of Process Control*, in press (1991).

Hildago, P. M., and C. B. Brosilow, "Nonlinear Model Predictive Control of Styrene Polymerization at Unstable Operating Points," *Comp. & Chem. Eng.*, **14**, 481 (1990).

Hirschorn, R. M., "Invertibility of Nonlinear Control Systems," *SIAM J. Cont. Optimiz.*, **17**, 289 (1979).

Hirschorn, R. M., "(A, B)-Invariant Distributions and Disturbances Decoupling of Nonlinear Systems," *SIAM J. Cont. Optimiz.*, **19**, 1 (1981).

Isidori, A., *Nonlinear Control Systems: An Introduction*, 2nd ed., Springer-Verlag, NY (1989).

Isidori, A., A. J. Krener, C. Gori Giorgi, and S. Monaco, "Nonlinear Decoupling via Feedback: A Differential Geometric Approach," *IEEE Trans. Auto Cont.*, **AC-26**, 331 (1981).

Johnson, A., "The Control of Fed-Batch Fermentation Processes—A Survey," *Automatica*, **23**, 691 (1987).

Joseph, B., and C. B. Brosilow, "Inferential Control of Processes," *AIChE J.*, **24**, 485 (1978).

Kailath, T., *Linear Systems*, Prentice-Hall, Englewood Cliffs, NJ (1980).

Kantor, J. C., "A Finite Dimensional Observer for an Exothermic Stirred-Tank Reactor," *Chem. Eng. Sci.*, **44**, 1503 (1989).

Kappos, E., "A Geometrical Linearization Theory," *Proc. IEEE Conf. on Decision and Control*, Las Vegas, 77 (1989).

Kravaris, C., "Input/Output Linearization: A Nonlinear Analog of Placing Poles at the Process Zeros," **34**, 1803 (1988).

Kravaris, C., and C. Chung, "Nonlinear State Feedback Synthesis by Global Input/Output Linearization," *AIChE J.*, **33**, 592 (1987).

Kravaris, C., and P. Daoutidis, "Nonlinear State Feedback Control of Second-Order Nonminimum-Phase Nonlinear Systems," *Comp. & Chem. Eng.*, **14**, 439 (1990).

Kravaris, C., and J. C. Kantor, "Geometric Methods for Nonlinear Process Control: I. Background," *Ind. Eng. Chem. Res.*, **29**, 2295 (1990a).

Kravaris, C., and J. C. Kantor, "Geometric Methods for Nonlinear Process Control: II. Controller Synthesis," *Ind. Eng. Chem. Res.*, **29**, 2311 (1990b).

Kravaris, C., and S. Palanki, "Robust Nonlinear State Feedback Under Structured Uncertainty," *AIChE J.*, **34**, 1119 (1988).

Lee, P. L., and G. R. Sullivan, "Generic Model Control (GMC)," *Comp. & Chem. Eng.*, **12**, 573 (1988).

Li, W. C., L. T. Biegler, C. G. Economou, and M. Morari, "A Constrained Pseudo-Newton Control Strategy for Nonlinear Systems," *Comp. & Chem. Eng.*, **14**, 451 (1990).

Lien, C.-Y., and T.-S. Wang, "Application of Feedback Linearization to Bioreactor Control," *Proc. Amer. Cont. Conf.*, San Diego, 2161 (1990).

Marino, R., and P. V. Kokotovic, "A Geometric Approach to Nonlinear Singularly Perturbed Control Systems," *Automatica*, **24**, 31 (1988).

Morari, M., and E. Zafiriou, *Robust Process Control*, Prentice Hall, Englewood Cliffs, NJ (1989).

Nikolaou, M., and V. Manousiouthakis, "A Hybrid Approach to Nonlinear System Stability and Performance," *AIChE J.*, **35**, 559 (1989).

Parrish, J. R., and C. B. Brosilow, "Nonlinear Inferential Control of Reactor Effluent Concentration from Temperature and Flow Measurements," *Proc. Amer. Cont. Conf.*, Seattle, 1027 (1986).

Parrish, J. R., and C. B. Brosilow, "Nonlinear Inferential Control," *AIChE J.*, **34**, 633 (1988).

Saberi, A., P. V. Kokotovic, and H. J. Sussmann, "Global Stabilization of Partially Linear Composite Systems," *SIAM J. Cont. and Optim.*, **28**, 1491 (1990).

Sussmann, H. J., "Limitations of the Stabilizability of Globally Minimum Phase Systems," *IEEE Trans. Auto. Control*, **AC-35**, 117 (1990).

Sussmann, H. J., and P. V. Kokotovic, "The Peaking Phenomenon and the Global Stabilization of Nonlinear Systems," *IEEE Trans. Auto. Cont.*, **AC-36**, 424 (1991).

Appendix

Proof of theorem 1

To compare the IMC controllers in Eqs. 44 and 51, a state-space realization of the transfer function in Eq. 41 is required.

A particularly convenient minimal realization of $G(s)$ is the companion form (Kailath, 1980; Isidori, 1989):

$$\tilde{A} = \begin{bmatrix} 0 & 1 & 0 & \cdots & 0 \\ 0 & 0 & 1 & \cdots & 0 \\ \cdot & \cdot & \cdot & \cdots & \cdot \\ 0 & 0 & 0 & \cdots & 1 \\ -\tilde{a}_0 & -\tilde{a}_1 & -\tilde{a}_2 & \cdots & -\tilde{a}_{n-1} \end{bmatrix} \quad \tilde{B} = \begin{bmatrix} 0 \\ 0 \\ \cdot \\ 0 \\ \tilde{K} \end{bmatrix} \quad (A1)$$

$$\tilde{C} = [\tilde{b}_0 \ \tilde{b}_1 \ \cdots \ \tilde{b}_{n-r-1} \ 1 \ 0 \ \cdots \ 0] \quad (A2)$$

We first show that the model inverse controllers in Eqs. 42 and 50 obtained from the transfer function and state-space approaches, respectively, have identical input-output behavior. The following relationship between the state variables can be obtained from the $\tilde{A}$ matrix in Eq. A1:

$$\tilde{x}_k(s) = s^{k-1} \tilde{x}_1(s) \quad 2 \leq k \leq n \quad (A3)$$

From Eq. A2 it follows that:

$$\tilde{y}(s) = [\tilde{b}_0 + \tilde{b}_1 s + \cdots$$
$$+ \tilde{b}_{n-r-1} s^{n-r-1} + s^{n-r}] \tilde{x}_1(s) = \tilde{b}(s) \tilde{x}_1(s) \quad (A4)$$

Hence, the state $\tilde{x}_1$ is related to the input u as:

$$\tilde{x}_1(s) = \frac{1}{\tilde{b}(s)} \tilde{K} \frac{\tilde{b}(s)}{\tilde{a}(s)} u(s) = \tilde{K} \frac{1}{\tilde{a}(s)} u(s) \quad (A5)$$

Using the state-space realization in Eqs. A1 and A2, the derivatives in Eqs. 47 and 48 have the form:

$$\tilde{y}^{(k)} = \tilde{b}_0 \tilde{x}_{k+1} + \tilde{b}_1 \tilde{x}_{k+2} + \cdots$$
$$+ \tilde{b}_{n-r-1} \tilde{x}_{n-r+k} + \tilde{x}_{n-r+k+1} \quad 1 \leq k \leq r-1 \quad (A6)$$

$$\tilde{y}^{(r)} = \tilde{b}_0 \tilde{x}_{r+1} + \tilde{b}_1 \tilde{x}_{r+2} + \cdots + \tilde{b}_{n-r-1} \tilde{x}_n - \tilde{a}_0 \tilde{x}_1$$
$$- \tilde{a}_1 \tilde{x}_2 - \cdots \tilde{a}_{n-1} \tilde{x}_n + \tilde{K} u \quad (A7)$$

From Eqs. A3 and A7 it follows that:

$$s^r \tilde{y}(s) = [\tilde{b}_0 s^r + \tilde{b}_1 s^{r+1} + \cdots + \tilde{b}_{n-r-1} s^{n-1}] \tilde{x}_1(s)$$
$$- [\tilde{a}_0 + \tilde{a}_1 s + \cdots + \tilde{a}_{n-1} s^{n-1}] \tilde{x}_1(s) + \tilde{K} u$$
$$= s^r [\tilde{b}(s) - s^{n-r}] \tilde{x}_1(s) - [\tilde{a}(s) - s^n] \tilde{x}_1(s) + \tilde{K} u$$
$$= [s^r \tilde{b}(s) - \tilde{a}(s)] \tilde{x}_1(s) + \tilde{K} u \quad (A8)$$

The Laplace transform of the model inverse controller in Eq. 50 with zero initial conditions can be obtained by setting the righthand side of Eq. A8 equal to $s^r v(s)$ and solving for $u(s)$:

$$u(s) = -\frac{s^r \tilde{b}(s) - \tilde{a}(s)}{\tilde{K}} \tilde{x}_1(s) + \frac{1}{\tilde{K}} s^r v(s) \quad (A9)$$

Equation A5 can be used to eliminate $\tilde{x}_1(s)$:

$$u(s) = [\tilde{a}(s) - s^r \tilde{b}(s)] \frac{1}{\tilde{a}(s)} u(s) + \frac{1}{\tilde{K}} s^r v(s) \quad (A10)$$

If Eq. A10 is solved for $u(s)$, Eq. 42 is obtained. Since the result is independent of the state-space realization, the model inverse controllers obtained from the transfer function and state-space design strategies have identical input-output behavior.

We now show that the filters in Eqs. 43 and 49, obtained from the transfer function and state-space approaches, respectively, have identical input-output behavior. Let a polynomial $\alpha(s)$ be defined as:

$$\alpha(s) \triangleq s^r + \alpha_r s^{r-1} + \cdots + \alpha_2 s + \alpha_1 \quad (A11)$$

Then by using Eq. 47, the Laplace transform of the filter in Eq. 49 with zero initial conditions can be written as:

$$s^r v(s) = [s^r - \alpha(s)] \tilde{y}(s) + \alpha_1 e(s) \quad (A12)$$

Using Eqs. 41 and 42, the filter can be represented as:

$$v(s) = \frac{\alpha_1}{\alpha(s)} e(s) \quad (A13)$$

The filter tuning parameters $\{\alpha_1\}$ can be chosen (Henson and Seborg, 1990b) to yield the transfer function in Eq. 43. Since the result is independent of the state-space realization, the filters obtained from the transfer function and state-space design strategies have identical input-output behavior. Thus, the IMC controllers Q derived from the transfer function and state-space design strategies have identical input-output behavior and have the form in Eq. 44. □

Proof of theorem 2

Since the condition in Eq. 26 is satisfied by assumption, the CLTF in Eq. 34 holds. If $\epsilon = 0$, Eq. 34 reduces to:

$$\tilde{y}(t) = e(t) = r(t) - y(t) + \tilde{y}(t) \quad (A14)$$

Because $\tilde{y}(t)$ is bounded by assumption, perfect control [i.e., $y(t) = r(t) \ \forall \ t \geq 0$] is obtained as claimed. We now show that if $\epsilon = 0$, the IMC controller Q in Eq. 30 reduces to the model inverse controller in Eq. 20 with $e^{(r)}$ as the input. Using Eqs. 1, 29, and A14, the closed-loop system can be represented as follows if $\epsilon = 0$:

$$\dot{\tilde{x}} = \tilde{f}(\tilde{x}) - \tilde{g}(\tilde{x}) \frac{L_{\tilde{f}}^r \tilde{h}(\tilde{x})}{L_{\tilde{g}} L_{\tilde{f}}^{r-1} \tilde{h}(\tilde{x})} + \frac{\tilde{g}(\tilde{x})}{L_{\tilde{g}} L_{\tilde{f}}^{r-1} \tilde{h}(\tilde{x})} v^{(r)} \quad (A15)$$

$$e = \tilde{h}(\tilde{x}) \quad (A16)$$

Taking the first time derivative of e yields:

$$\dot{e} = L_f \tilde{h}(\tilde{x}) - L_g \tilde{h}(\tilde{x}) \frac{L_f^r \tilde{h}(\tilde{x})}{L_g L_f^{r-1} \tilde{h}(\tilde{x})}$$

$$+ L_g \tilde{h}(\tilde{x}) \frac{1}{L_g L_f^{r-1} \tilde{h}(\tilde{x})} v^{(r)} = L_f \tilde{h}(\tilde{x}) \quad \text{(A17)}$$

since $L_g \tilde{h}(\tilde{x}) = 0$ by assumption 3. The second derivative of e is:

$$\ddot{e} = L_f^2 \tilde{h}(\tilde{x}) - L_g L_f \tilde{h}(\tilde{x}) \frac{L_f^r \tilde{h}(\tilde{x})}{L_g L_f^{r-1} \tilde{h}(\tilde{x})}$$

$$+ L_g L_f \tilde{h}(\tilde{x}) \frac{1}{L_g L_f^{r-1} \tilde{h}(\tilde{x})} v^{(r)} = L_f^2 \tilde{h}(\tilde{x}) \quad \text{(A18)}$$

since $L_g L_f \tilde{h}(\tilde{x}) = 0$ by assumption 3. The procedure can be continued to show that:

$$e^{(k)} = L_f^k \tilde{h}(\tilde{x}) \quad 1 \le k \le r - 1 \quad \text{(A19)}$$

Thus, the rth derivative is:

$$e^{(r)} = L_f^r \tilde{h}(\tilde{x}) - L_g L_f^{r-1} \tilde{h}(\tilde{x}) \frac{L_f^r \tilde{h}(\tilde{x})}{L_g L_f^{r-1} \tilde{h}(\tilde{x})}$$

$$+ L_g L_f^{r-1} \tilde{h}(\tilde{x}) \frac{1}{L_g L_f^{r-1} \tilde{h}(\tilde{x})} v^{(r)} = v^{(r)} \quad \text{(A20)}$$

Hence, the IMC controller Q in Eq. 30 reduces to the model inverse controller in Eq. 20 with $e^{(r)}$ as the input. The model inverse controller is well defined by assumption 2. □

Proof of theorem 3

By assumption 1, the plant is identical to the model. Hence, the objective is to show that the control law in Eq. 30 yields a stable closed-loop system when applied to the model (plant) in Eq. 1. Using assumptions 2 and 3, it can be shown that there exists a nonlinear change of coordinates such that the closed-loop system comprising Eqs. 1 and 30 can be represented as follows (Henson and Seborg, 1991),

$$\dot{\xi} = \begin{bmatrix} 0 & 1 & 0 & \cdots & 0 \\ 0 & 0 & 1 & \cdots & 0 \\ \cdot & \cdot & \cdot & \cdots & \cdot \\ 0 & 0 & 0 & \cdots & 1 \\ -\alpha_1 & -\alpha_2 & -\alpha_3 & \cdots & -\alpha_r \end{bmatrix} \xi + \begin{bmatrix} 0 \\ 0 \\ \cdot \\ 0 \\ \alpha_1 \end{bmatrix} y_{sp} \quad \text{(A21)}$$

$$\tilde{y} = [1 \ 0 \ \cdots \ 0 \ 0]\xi \quad \text{(A22)}$$

$$\dot{\eta} = q(\xi, \eta) \quad \text{(A23)}$$

where ξ and η are new r-dimensional and $(n-r)$-dimensional state vectors, respectively.

The characteristic polynomial of Eq. A21 is $\alpha(s)$ in Eq. A11. Since $\epsilon > 0$ by assumption, $\alpha(s)$ is Hurwitz (Henson and Seborg, 1990c). Thus, the ξ state variables are bounded because y_{sp} is assumed to be bounded. Since the ξ state variables are bounded, the η state variables are bounded by assumption 5. The boundedness of the ξ and η state variables and assumption 2 imply that the original $\tilde{x}$ state variables are bounded (Isidori, 1989). The output $\tilde{y}$ is bounded by Eq. A22. By assumption 2, the functions $L_f^k \tilde{h}(\tilde{x})$, $k \ge 0$, are bounded. Hence, $v^{(r)}$ in Eq. 28 is bounded because $e = y_{sp}$ by assumption 1 and y_{sp} is bounded. By assumption 3, the function $L_g L_f^{r-1} \tilde{h}(\tilde{x})$ is bounded away from zero. Thus, u in Eq. 29 is bounded. Hence, all signals are bounded and the closed-loop system is internally and input-output stable. □

Proof of theorem 4

Because the closed-loop system is asymptotically stable by assumption:

$$\lim_{t \to \infty} \tilde{y}^{(k)}(t) = 0 \quad \forall \ k \ge 1 \quad \text{(A24)}$$

It follows from Eqs. 15 and 16 that in the limit as $t \to \infty$:

$$L_f^k \tilde{h}(\tilde{x}) = 0 \quad 1 \le k \le r - 1 \quad \text{(A25)}$$

$$L_f^r \tilde{h}(\tilde{x}) + L_g L_f^{r-1} \tilde{h}(\tilde{x}) u(t) = 0 \quad \text{(A26)}$$

Hence, $v^{(r)}(t) = 0$ in the limit as $t \to \infty$ by Eq. 29. From Eq. 28 it follows that in the limit as $t \to \infty$:

$$-\alpha_1 \tilde{h}(\tilde{x}) + \alpha_1 e = 0 \quad \text{(A27)}$$

By the definition of $\tilde{h}(\tilde{x})$ in Eq. 2 and e in Eq. 5, it follows that:

$$\lim_{t \to \infty} [y(t) - y_{sp}(t)] = 0 \quad \text{(A28)}$$

Hence, the control law in Eq. 30 eliminates offset. □

Proof of theorem 5

By assumption, the model and plant dynamics in Eqs. 1 and 2, respectively, are identical except for the initial conditions. Since $u(t) = u_o \ \forall \ t \ge 0$ by assumption, the dynamics can be represented as:

$$\dot{x} = f(x) + g(x)u_o \triangleq F(x), \quad x(0) = x_o \quad \text{(A29)}$$

$$\dot{\tilde{x}} = f(\tilde{x}) + g(\tilde{x})u_o \triangleq F(\tilde{x}), \quad \tilde{x}(0) = \tilde{x}_o \quad \text{(A30)}$$

where $\tilde{x}_o \neq x_o$. Without loss of generality, assume that $x_o = 0$ is an equilibrium point of Eq. A29. Then, $x(t) = 0 \ \forall \ t \geq 0$ by assumption 4. If the state estimation error is defined as $e_x \triangleq \tilde{x} - x$, the error dynamics are:

$$\dot{e}_x = \dot{\tilde{x}} - \dot{x} = F(\tilde{x}) = F(e_x + x) = F(e_x) \qquad \text{(A31)}$$

By assumption 4, 0 is a globally asymptotically stable equilib-rium point of the error dynamics in Eq. A31. Hence, the state estimation error decays asymptotically to zero,

$$\lim_{t \to \infty} \| \tilde{x}(t) - x(t) \| = 0 \qquad \text{(A32)}$$

as claimed. □